JOURNAL OF MATERIALS SCIENCE: MATERIALS IN MEDICINE **16** (2005) 491 – 501

Towards a medically approved technology for alginate-based microcapsules allowing long-term immunoisolated transplantation

H. ZIMMERMANN[1], D. ZIMMERMANN[2], R. REUSS[3], P. J. FEILEN[4], B. MANZ[5], A. KATSEN[1], M. WEBER[3], F. R. IHMIG[1], F. EHRHART[1], P. GEßNER[3], M. BEHRINGER[3], A. STEINBACH[3], L. H. WEGNER[3], V. L. SUKHORUKOV[3], J. A. VÁSQUEZ[6], S. SCHNEIDER[7], M. M. WEBER[4], F. VOLKE[5], R. WOLF[8], U. ZIMMERMANN[3,*]

[1]Abteilung Kryobiophysik & Kryotechnologie, Fraunhofer-Institut für Biomedizinische Technik, 66386 St. Ingbert, Germany
[2]Abteilung für Biophysikalische Chemie, Max-Planck-Institut für Biophysik, 60439 Frankfurt, Germany
[3]Lehrstuhl für Biotechnologie, Biozentrum, Universität Würzburg, 97074 Würzburg, Germany
E-mail: zimmerma@biozentrum.uni-wuerzburg.de
[4]Schwerpunkt Endokrinologie und Stoffwechselerkrankungen, Medizinische Klinik und Poliklinik, Universitätsklinik Mainz, 55131 Mainz, Germany
[5]Arbeitsgruppe Magnetische Resonanz, Fraunhofer-Institut für Biomedizinische Technik, 66386 St. Ingbert, Germany
[6]Depto. Biologia Marina, Facultad de Ciencias del Mar, Universidad Catolica del Norte, Coquimbo, Chile
[7]Allgemeine Innere Medizin, Endokrinologie und Diabetologie, Berufsgenossenschaftliche Kliniken Bergmannsheil, Universitätsklinik Bochum, 44789 Bochum, Germany
[8]Lehrstuhl für Zoologie I, Elektronenmikroskopie, Biozentrum, Universität Würzburg, 97074 Würzburg, Germany

The concept of encapsulated-cell therapy is very appealing, but in practice a great deal of technology and know-how is needed for the production of long-term functional transplants. Alginate is one of the most promising biomaterials for immunoisolation of allogeneic and xenogeneic cells and tissues (such as Langerhans islets). Although great advances in alginate-based cell encapsulation have been reported, several improvements need to be made before routine clinical applications can be considered. Among these is the production of purified alginates with consistently high transplantation-grade quality. This depends to a great extent on the purity of the input algal source as well as on the development of alginate extraction and purification processes that can be validated. A key engineering challenge in designing immunoisolating alginate-based microcapsules is that of maintaining unimpeded exchange of nutrients, oxygen and therapeutic factors (released by the encapsulated cells), while simultaneously avoiding swelling and subsequent rupture of the microcapsules. This requires the development of efficient, validated and well-documented technology for cross-linking alginates with divalent cations. Clinical applications also require validated technology for long-term cryopreservation of encapsulated cells to maintaining a product inventory in order to meet end-user demands. As shown here these demands could be met by the development of novel, validated technologies for production of transplantation-grade alginate and microcapsule engineering and storage. The advances in alginate-based therapy are demonstrated by transplantation of encapsulated rat and human islet grafts that functioned properly for about 1 year in diabetic mice.
© *2005 Springer Science + Business Media, Inc.*

*Author to whom all correspondence should be addressed.

1. Introduction

Treatment of hormone deficiency diseases, such as diabetes mellitus or hypoparathyroidism, by the transplantation of immunoisolated living cells or tissue fragments that release the therapeutic factors is a very appealing approach for overcoming the limitations of current therapies (see [1–4]). A matrix (e.g. cross-linked alginate) protects cells against the immune response of the host while simultaneously allowing unimpeded transfer of nutrients, oxygen, and therapeutic factors. This permits the imitation of moment-to-moment fine regulation of the missing therapeutic factors, avoids a lifetime of immunosuppressive therapy and allows the use of non-human cells (thus overcoming the limited supply of human donor cells). Small-scale clinical trials [3, 5] have given impressive evidence of the potential of encapsulated cell therapy. Transplantation of Ba^{2+}-alginate-encapsulated allogeneic parathyroid tissue pieces into the non-dominant forearm of patients with hypoparathyroidism demonstrated normocalcemia and normal levels of parathormone shortly after surgery. Without administration of any immunosuppressives the grafts functioned for over three months before failure. During this time the patients were free of symptoms of sequelae of hypoparathyroidism. Evaluation of the clinical data and of the numerous results obtained from animal studies using alginate and other matrices [1, 3] have shown that the biophysical, biochemical and immunological characteristics of the protectant (such as biocompatibility, size, permeability, mechanical strength, elasticity, surface topography, swelling characteristics etc.) must be carefully tuned to prevent functional loss of the transplant and matrix breakdown. However, the numerous matrix parameters cannot be adjusted independently [6]. Thus, seemingly minor modifications of one property can have important implications for others. A further problem is that the demands placed on an immunoisolating matrix may vary with the type of therapeutic application. A prerequisite for routine clinical application that has so far not been addressed is also the necessity of delivering well-characterized grafts "on demand" or the "pooling" of grafts, which implies the need for preservation.

Recent work in our laboratories demonstrated that microcapsules of extremely high-viscosity alginate extracted in a novel way from sterilized algae and uniformly cross-linked with Ba^{2+} ions meet the various demands for a long-term immunoprotecting encapsulation matrix. The uniform gelling of alginate produces very stable microcapsules and is achieved by the injection of $BaCl_2$ crystals into the cores of the microcapsules before they come into contact with external Ba^{2+} [7]. Application of the so-called "crystal gun" technique allows reproducible cross-linking even for large-sized microcapsules (about 1 mm). Not only does this increase the efficiency of the process, it also minimizes the risk of capsule damage during transplantation. The "crystal gun" method also allows the fine-tuning of microcapsule parameters for factor delivery independent of the alginate composition and nature of the encapsulated cell/tissue. This leads to a robust and easy to validate protocol. Advanced technology is now also available for assessing of the quality of the alginate and the uniformity of the (surface and bulk) cross-linking.

These recent developments have paved the way for xenografts functional for about 1 year in rodents. In the light of these encouraging results together with improvements in the storage of cells and tissues (cryopreservation), clinical trials are obviously justified in the near future. It is within the realms of possibility that the whole process can be optimized under "Good Manufacturing Practice" (GMP) conditions.

2. Alginate source and characteristics

Alginates are found in brown algae and in bacterial species [8]. They consist of unbranched binary copolymers of 1-4 linked β-D-mannuronic acid (M) and α-L-guluronic acid (G), of widely varying composition and sequential structure (MMM-blocks, GGG-blocks and MGM-blocks). The alkali-, ammonium- and magnesium-alginates are soluble in water. Gelation of alginates occurs when the carboxyl groups of the polymers are cross-linked with multi-valent cations (e.g. Ca^{2+}, Ba^{2+}, La^{3+}, Fe^{3+}) and poly-electrolytes. Depending on the nature of the cross-linking cation, the length of the polymeric chains, the M:G ratio and the percentage of the block structures, hydrogels of varying mechanical strength, elasticity and swelling characteristics can be produced (for more details, see [4]). When cross-linked with Ba^{2+}, high-M alginates result in elastic microcapsules, whereas microcapsules based on high-G alginate exhibit high mechanical strength. Mixing of high-M and high-G alginates is an elegant way for designing microcapsules of desired strength and formability, particularly if such material is taken from algae of the same genus. Suitable algal sources for such alginate mixtures are *Lessonia nigrescens* (Fig. 1A) and *Lessonia trabeculata* (Fig. 1B). Both species grow from central Peru to southern Chile. *L. nigrescens* grows in the tidal zone and is exposed to strong surf. The stipes are very elastic and flexible because of high-M alginate (about 60%; [9]). In contrast, *L. trabeculata* occurs between 0 and 30 m in subtidal habitats and is exposed to heavy currents [10]. The stipes of this species are very stiff due to an extremely high content of G (about 90%; [11]).

3. Alginate extraction and purification technology

Crude commercial alginates are not recommended as starting materials as they contain many inorganic and organic impurities including non-natural constituents that would have to be removed. This is because dried algal material is washed ashore by the surf and the winds. This material is polluted with components of bacterial, fungal, animal and anthropogenic origin. Treatment of the raw algal material by formaldehyde causes further complications because of partially unknown interactions between alginate and impurities [3]. Commercial products can contain spores or components of gram-positive bacteria commonly occurring in marine environments (e.g. *Bacillus anthracis, Bacillus cereus* and *Bacillus thuringiensis*; [12]). Contamination by

Figure 1 Source of alginates: stipes of *Lessonia nigrescens* (A) and *Lessonia trabeculata* (B). Note that the stipes in (A) are very flexible because of high-M, while the stipes in (B) are mechanically very stiff due to high-G.

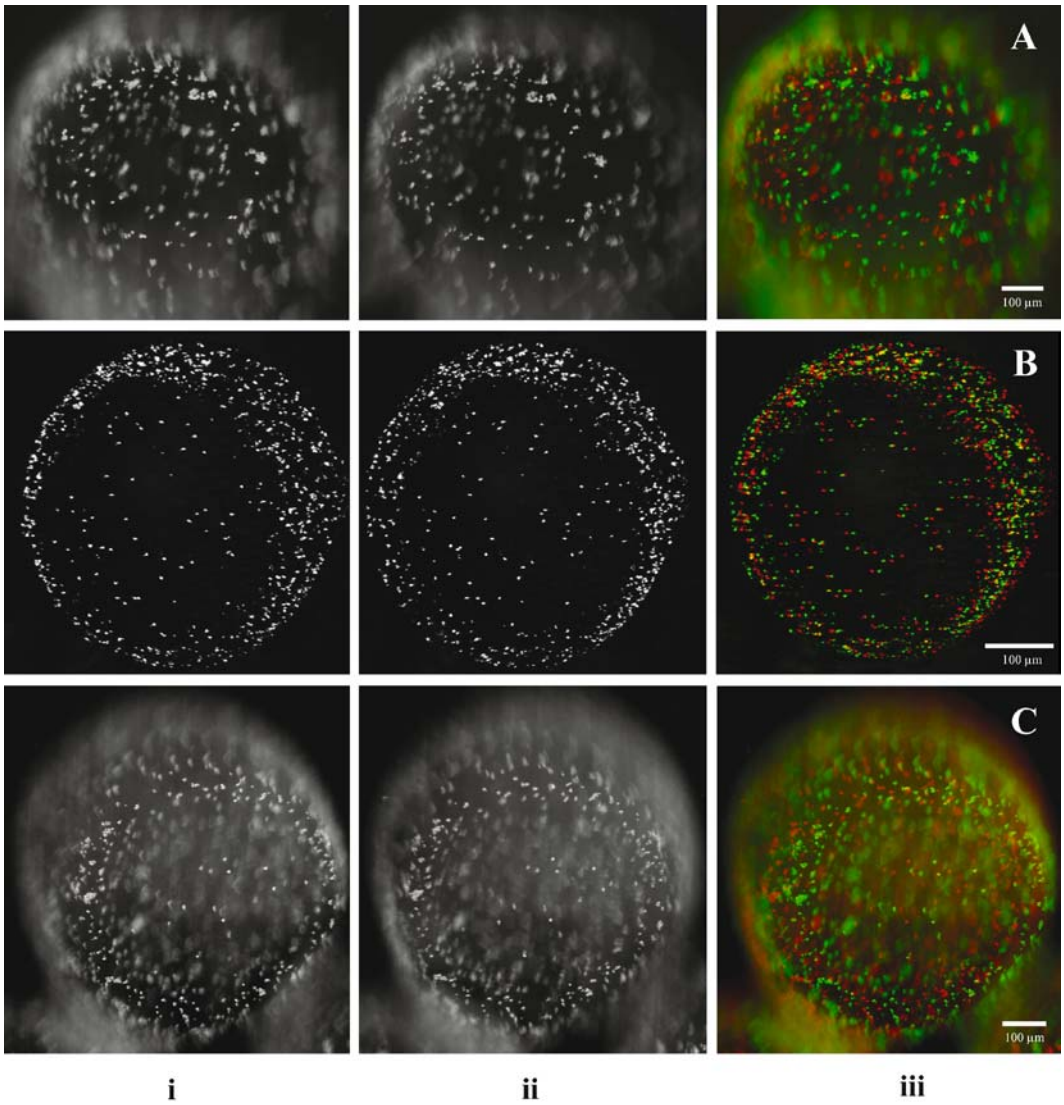

Figure 3 Stereo pair (i, ii) and anaglyphic 3-D image (iii) of microcapsules visualized by real-time 3-D dark field microscopy (A and C) and by CLSM (B; reconstructed from 64 optical sections). The microcapsules were made up of *L. nigrescens* alginate (0.8% w/v in A and 0.75% w/v in B and C) and cross-linked by external Ba^{2+} (A) and by the "crystal gun" method (B, C). Note that when fused by staring, the stereo pair (i and ii) shows a depth-reversed virtual view from the interior to the surface of the microcapsule (A, C). In (B) this virtual view is restricted to the 2nd quarter, otherwise the abundant crystals adhering to the outer surface of the microcapsule calotte would disturb the view on the crystals within the microcapsule. For viewing of the anaglyphic 3-D images (iii) red/green or red/blue glasses or filters must be used.

gram-positive debris has not received attention by workers in the field, but is extremely important for the production of biocompatible alginates. Furthermore, due to the harvesting and extraction process the viscosity (closely linked to the molecular weight) of commercial alginates is also rather low (1–5 mPa s; 0.1% w/v solution; [4]), enhancing the risk of graft failure since the cytotoxicity of polymers increases with decreasing molecular mass [13].

These disadvantages do not exist when fresh stipes of brown algae (free of overgrowth by epiphytes) are harvested directly from the sea, peeled and, most importantly, subjected to antimicrobial treatment. The products of subsequent extraction and purification can further be considerably improved when the surface of the stipe pieces are physically cleaned. This treatment removes immunogenic surface proteins of non-plant origin that are frequently found in alginates after extraction and purification. Alginate is extracted by using a mixture of appropriate Ca^{2+}-chelating agents and purified by repeated alcohol (or acetone) precipitation. Under these conditions, clinical-grade alginates of extremely high-viscosity (>30 mPa s; 0.1% w/v solution) can be routinely produced on a large scale. The basic operational steps are depicted in Fig. 2. Large-scale production has demonstrated that the process is very robust resulting in clinical-grade alginate. However, it should be noted that the various parameters of the production process are highly mutually dependent. The fine-tuning of the process has only been possible because of the introduction of new assays and technologies in the last two years. Using the monitoring technology, the extraction protocols depicted in Fig. 2 can be optimized relatively easily for each algal species.

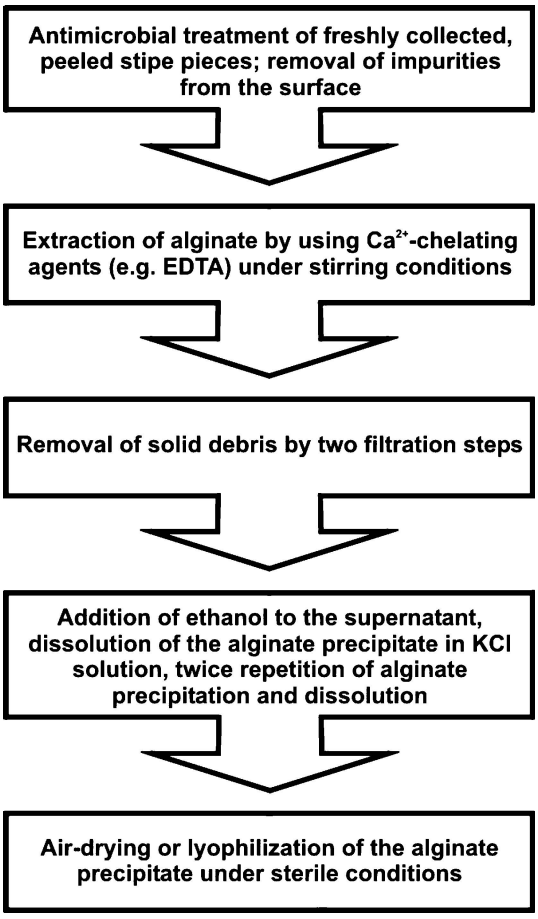

Figure 2 Flow chart for the extraction and purification of ultra-high-viscosity alginate from freshly collected, peeled stipes of *L. nigrescens* and *L. trabeculata*.

4. Alginate validation technology

The regulatory agencies will not approve a process unless it can be validated in a defined and documented manner. A key element of the validation of the alginate purification process is the monitoring of impurities and their removal by the process. The ASTM Standards for characterization and testing of alginates are of crucial relevance [14], but the analytical assays described there and elsewhere do not yield the information required for the prediction of the occurrence of foreign body reactions under transplantation conditions. Therefore, the quality of alginate (and other matrices used in immunoisolated transplantation) is usually assured by transplantation of the material into rodents [3, 4]. Most stringent small animal models are NOD mice [15] and spontaneously diabetic BB/OK rats (because of their elevated macrophage activity; [16]). Experience has shown [3] that the results obtained in these rodents can easily be extrapolated to the clinical situation in human beings without studies in large animals. The weakness of transplantation studies is that they are very expensive, time- and manpower-consuming. A further and very important drawback of animal studies is also the frequently very variable outcome. In some cases, microcapsules made up of the same purified alginate lot and implanted simultaneously beneath the right- and left-kidney capsule have shown quite different responses. Even microcapsules implanted under the same kidney sometimes induce a different response.

As shown recently [12], the transplantation-grade quality of alginates can be reliably predicted by a cell assay based on the induction of apoptosis in Jurkat cells. This assay in combination with the "modified mixed lymphocyte" assay introduced by Zimmermann *et al.* [17] allows rapid and highly sensitive screening for any fibrosis-inducing impurities in alginate samples, even during the purification regime. These assays fulfill the demand for safety standards of large-scale alginate production and should, therefore, be mandatory for the commercial manufacture of alginate for clinical trials.

5. Microcapsule design technology and validation

Alginate microcapsules are usually produced by dropping cell-loaded alginate into solutions containing 20 mM Ca^{2+} or Ba^{2+} using a 2- or 3-channel air-jet droplet generator [4]. Cross-linking the carboxyl groups of M and G with Ba^{2+} rather than Ca^{2+} considerably increases the mechanical stability of the microcapsules. However, the Ba^{2+} has to be removed after 15 min incubation to prevent both continuing inhibition of K^+ channels in the membrane of encapsulated cells (leading to cell death) as well as initial swelling of the microcapsules due to the osmotic pressure exerted by Ba^{2+} ([18, 19] and literature quoted there). Removal of excess Ba^{2+} is achieved by several washing steps with

isotonic NaCl solution followed by a sulfate treatment to precipitate any remaining free Ba^{2+} ions. Swelling of the microcapsules under transplantation conditions and thus mechanical instability can be delayed further when proteins (e.g. up to 3% human serum albumin; HSA) are added to the alginate solution before microcapsule formation [20, 21]. However, swelling and breakage of microcapsules can still occur after long *in vitro* incubations as well as after long-term transplantation times [22]. One major reason for microcapsule swelling is the formation of concentration gradients of alginate polymers and/or of proteins incorporated for stabilization resulting in microdomains of different composition. Alginate polymer and protein concentration gradients arise from demixing and shrinking processes during droplet formation and gelling by external Ba^{2+} (see e.g. [23, 24]). The extent of these problems depends on microcapsule dimensions, the M:G ratio, the viscosity (and thus the average molecular mass) as well as on the molecular mass distribution of the alginate. The presence of non-gelling salts such as NaCl, the time of cross-linking and the spatial distribution of the cells play also an important role. Compared to commercial low-viscosity alginates these problems are less for ultra-high viscosity alginates extracted from freshly harvested, peeled stipes. But the problem remains that a cross-linking time of 15 min (dictated by cell physiology) is too short for equilibration of external Ba^{2+} between the core of the viscous alginate droplet and the external medium.

This has been demonstrated by the imaging of microcapsules (made from alginate extracted from *L. pallida* and cross-linked with Ba^{2+} for 15 min) with confocal laser scanning microscopy (CLSM) [7]. In order to visualize the distribution of Ba^{2+}, the excess ions were not removed by washing before sulfate treatment. Solid $BaSO_4$ particles appeared as white spots under the CLSM reflection mode (see also further below). As shown by H. Zimmermann *et al.* [7] many $BaSO_4$ crystals were attached to the surface of the conventionally cross-linked alginate/protein microcapsule forming a rather continuous peripheral layer. In contrast, there were very few crystals within the interior of the microcapsules indicating that diffusion of Ba^{2+} into the core was apparently restricted.

This finding is confirmed by a novel real-time 3-D dark field microscopy technique (Wolf, unpublished results, see also [25, 26]) that provides a true 3-D image at magnifications between 25:1 and 400:1 and can be used as an elegant tool for routine control of microcapsule quality. Similar to conventional 3-D techniques in single-lens light microscopy [25, 26] the microscope must be equipped with three polarizing filters: an L-form double polarizing filter mounted at the backward focal plane of the objective lens and one polarizer in both of the eyepieces. They serve as image switches and provide the left eye with the microscopic image formed by the left half of the objective lens, and *vice versa*. The unavoidable limitation of depth of focus is overcome by continuously focussing through the specimen. A typical stereo pair and the corresponding anaglyphic 3-D image of a microcapsule cross-linked with external Ba^{2+} and visualized by real-time 3-D dark field microscopy is given in Fig. 3A. Focussing through the entire microcapsule shows that only a very few, randomly distributed $BaSO_4$ crystals are found within the interior of the microcapsule.

As demonstrated recently by Manz *et al.* [24] advanced ^1H nuclear magnetic resonance (NMR) imaging also yields information about the quality of cross-linking within the interior of microcapsules. Ba^{2+}-cross-linked microcapsules are placed in NMR tubes containing a saline solution to which paramagnetic Cu^{2+} ions as contrast agent are added. Cu^{2+} diffusion and accumulation within the microcapsules is resolved and quantified by taking spatially resolved maps of the spin-lattice relaxation time T_1 and/or of the spin-spin relaxation time T_2. The T_1 and T_2 values of microcapsules bathed for up to 20 h in Cu^{2+}-containing medium are significantly lower than the corresponding values of the surrounding due to accumulation of the paramagnetic Cu^{2+} ions within the microcapsules (see further below Fig. 5). Cu^{2+} has a similar affinity constant to alginate as Ba^{2+} [27]. After washing with Cu^{2+}-free 0.9% NaCl solution, the T_1 and T_2 relaxation times of the microcapsules (spatially resolved) are identical to the corresponding values before the addition of Cu^{2+} to the system. This implies that binding of Cu^{2+} to charged or polar groups of the alginate (and the proteins) is very unlikely.

Evaluation of the T_1 and T_2 values of the microcapsules after washing has shown [24] that conventional cross-linking with external Ba^{2+} at a physiological pH value is frequently not complete. It is subject to large variations, even if the microcapsule production parameters (such as monomer composition, size of the microcapsules, time of exposure to Ba^{2+} etc.) are kept constant ([24] and unpublished data). Cross-linking in the peripheral layer of the microcapsules apparently restricts diffusion of Ba^{2+} ions into the microcapsule interior, thus preventing complete cross-linking.

Predictable and reproducible results are expected when external gelling is simultaneously accompanied by internal gelling. A possible strategy for achieving uniform gelling is to add photo-releasable, caged Ba^{2+} to the alginate solution before dropping [20]. The caged ions are not reactive, but free, reactive ions can be released by UV-irradiation of the droplets in the $BaCl_2$ solution. The disadvantage of this approach is that the released organic cage compounds will not receive transplantation approval. Another possible way is to incorporate tiny $BaCO_3$ crystals into the alginate/cell suspension and to perform the gelling process in the $BaCl_2$ solution at lower pH, liberating Ba^{2+} ions [28]. Other methods such as the incorporation of Ba^{2+}-containing thermally unstable liposomes [29] or the addition of antigelling cations [27] have also not resulted in long-term stable microcapsules. Best results have been obtained by the "crystal gun" method [7]. With this technique, dried, sterilized, tiny $BaCl_2$ crystals[1] are injected

[1]Nanosized crystals of $BaSO_4$ which are very reactive because of their large surface to volume ratio can also be used and may lead to an enhanced, and even more homogeneous gelling (unpublished results).

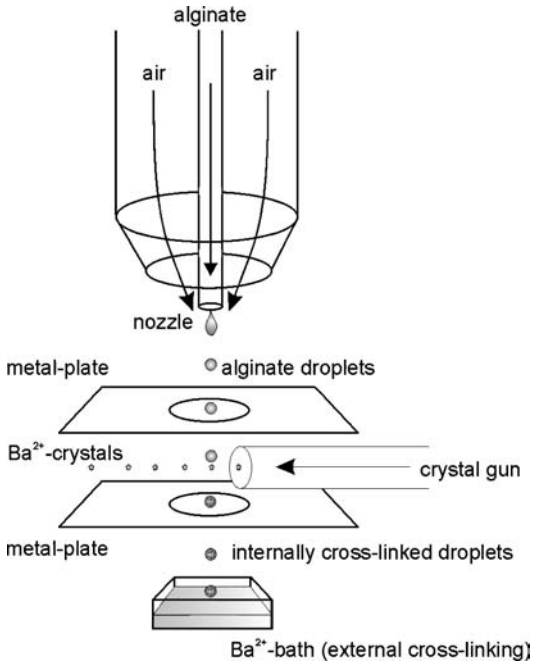

Figure 4 Schematic diagram of the "crystal gun" setup consisting of an air-jet droplet generator and a $BaCl_2$ crystal injector arranged perpendicularly to the droplet stream.

by air pressure into the alginate droplets shortly before they come into contact with the $BaCl_2$ solution (Fig. 4).

CLSM and 3-D dark field microscopy stereo pairs taken at different focal levels of microcapsules that were treated immediately with sulfate after cross-linking show (Fig. 3B and C) that $BaSO_4$ precipitates are distributed throughout the microcapsules. The number of precipitates depends both on crystal jet parameters (speed, crystal density etc.) and on the M:G ratio of the alginate used for encapsulation. For example, if the crystal jet parameters being appropriate for cross-linking of high-M alginate are applied to high-G alginates fewer crystals are found throughout the microcapsules. This effect is most likely due to the enhanced binding of Ba^{2+} to G-residues (which results in the so-called egg-box model; [27]). Consistent with the CLSM and 3-D dark field microscopy findings, T_2-^{1}H-NMR images (Fig. 5) confirm these findings, but additionally show that proteins must be incorporated in order to achieve complete occupation of the negatively charged groups of the alginate network within a 15-min incubation with Ba^{2+}.

Atomic force microscopy (AFM) images of microcapsules prepared with the "crystal gun" method have given no evidence of surface imperfections provided that excess Ba^{2+} ions are removed by several washing steps with saline solutions [7]. This finding is very important in the light of future clinical trials because smooth surfaces of highly purified Ba^{2+}-cross-linked alginate prevents the attachment, spreading and migration of fibroblasts or other anchorage-dependent cells [4]. This is shown by model experiments in which attachment of mouse fibroblasts on Ba^{2+}-cross-linked, planar films of alginate extracted from *L. nigrescens* were studied (Fig. 6). In order to enhance the adhesion properties of the purified alginate, 0.00125% fibronectin was incorporated into the

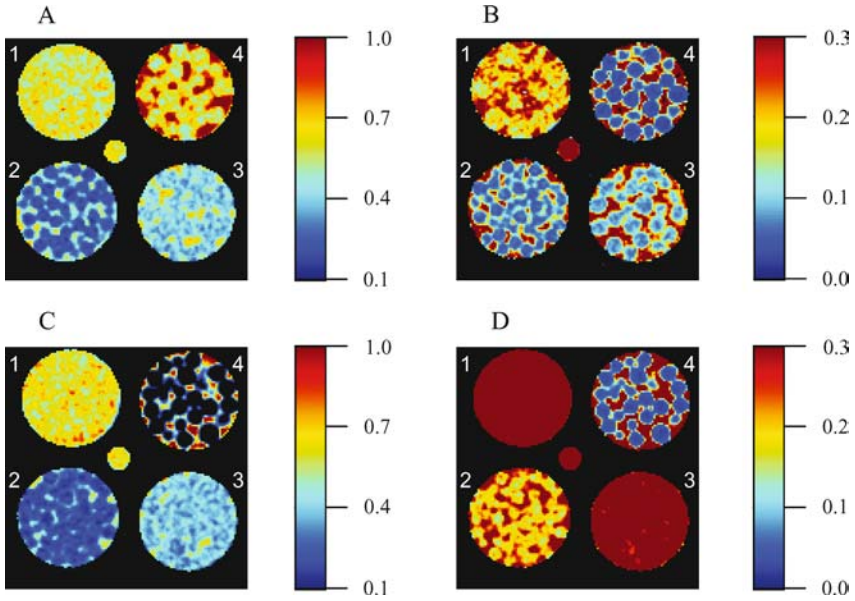

Figure 5 ^{1}H-NMR maps of the corresponding T_2 values of microcapsules made up of 0.65% w/v alginate and cross-linked with Ba^{2+} by using the "crystal gun" method. Source of alginates in A-D: (1) *L. nigrescens*; (2) *L. trabeculata*; (3 and 4) 1:1 mixtures of alginates extracted from *L. nigrescens* and *L. trabeculata*. Microcapsules 1–3, but not 4 (anti-clockwise, starting from top left) were stabilized with 10% fetal calf serum (FCS; is used instead of human serum albumin (HSA) because of precipitation of HSA by Cu^{2+}). Microcapsules were treated with 6 mM Na_2SO_4 for removal of excess Ba^{2+}. For recording of the T_2 maps microcapsule pellets were re-suspended in saline solution. The colored scale of the images represents the local T_2 value (given in seconds). T_2 maps are given before (A) and after 5 h (B) incubation in a 1.4 mM $CuSO_4$ solution. C and D represent the microcapsules washed with $CuSO_4$-free saline solution after 20 h incubation with $CuSO_4$. Note that the results of the washing process are given in different scales (C = colored scale as in A; D = colored scale as in B). Inspection of the controls in A shows that 2 and 3 are more tightly cross-linked than 1 and 4. Sample 1, but not the other samples, swells upon addition of Cu^{2+} (B-D). Accumulation of Cu^{2+} within the microcapsules assumes maximum values in 4, less in 2 and 3 and much less in 1. Furthermore, comparison of samples 1–3 in A and C, and sample 4 in B and D shows that Cu^{2+} can only be removed by washing if proteins are incorporated (1–3) indicating that proteins facilitate binding of Ba^{2+}. The small capillary in the centre of A-D filled with 1.4 mM Cu^{2+}-containing saline solution serves as a reference.

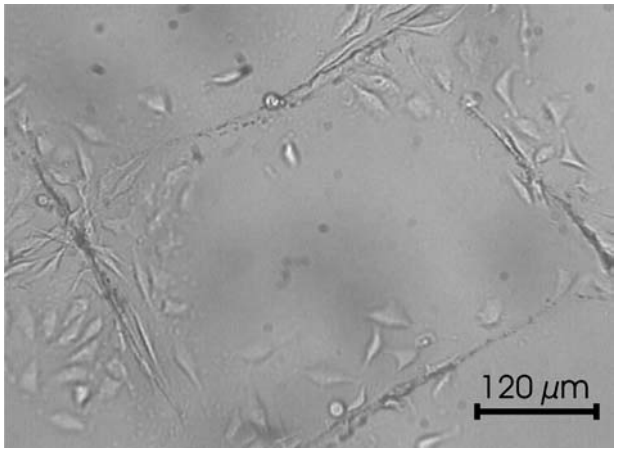

Figure 6 Adhesion and spreading of mouse fibroblasts on a planar, microstructured alginate film. The film was made by Ba^{2+}-cross-linking of highly purified *L. nigrescens* alginate (0.7% w/v in 0.9% NaCl solution containing 0.00125% fibronectin) on a glass substrate. Longitudinal imperfections (slots) were mechanically introduced by lightly pressing a metal grid into the gelled alginate film. Then the film was air-dried and re-hydrated in culture medium before fibroblasts were added. Note that fibroblast attachment, spreading and migration initially occurs preferentially along the imperfections even though the adhesivity of the alginate was enhanced by the addition of fibronectin.

matrix before gelling with external Ba^{2+}. When elongated crevices (or cracks) were mechanically introduced into the matrix, fibroblast attachment initially only occurred at these surface imperfections before (very delayed) spreading and migration of the cells over the entire surface of the planar film. Such processes are also expected under transplantation conditions. The alginate surface becomes more adhesive when anchorage-dependent cells attached to crevices or cracks start to migrate, thereby releasing cellular and membrane material. These materials together with advanced glycation end products (AGEs) (arising from non-enzymatic reactions of the polysaccharides; [30]) are immunogenic. "Topographical" biocompatibility is obviously equally important as "chemical" biocompatibility.

Microcapsules made up of alginates and alginate mixtures extracted from *L. pallida*, *L. nigrescens* and *L. trabeculata* incubated in 0.9% NaCl solution show a dramatic increase in stability when cross-linked by the "crystal gun" method as proved by incubation in 0.9% NaCl solution. In contrast to conventional cross-linking (unpublished results), microcapsules of high-G alginate extracted from *L. trabeculata* as well as 1:1 mixtures of this alginate with high-M alginate extracted from *L. nigrescens* are still stable after 36 weeks of incubation despite heavy stirring; the experiments are still continuing. There is also evidence that the amount of HSA (or FCS) added to the alginate for prevention of swelling can be reduced if pure G-rich or 1:1 mixtures of G-rich and M-rich alginates are used because of the very efficient cross-linking process. Complete omission of protein, however, is not advantageous because of incomplete cross-linking (see above and Fig. 5C and D) and deleterious effects on cellular function and integrity occur without HSA.

The crystal bombardment does not affect the viability and function of encapsulated cells and islets [7, 21]. However, it is important to note, that concomitant with the improvement of the cross-linking process, a decrease in permeability occurs that requires careful adjustment of the alginate concentration. For example, long-term viability and insulin secretion of islets decreased dramatically when 0.7% w/v instead of 0.65% w/v alginate extracted from *L. pallida* was used [21].

Unimpeded exchange of factors and nutrients between the microcapsules and the environment is only expected if pores exist in the alginate matrix. The existence of such pores can be shown by water permeability studies through 1-mm thick 2-D Ba^{2+}-cross-linked alginate membranes. Transmembrane water flows can be measured by the two-compartment setup in the inset of Fig. 7. If an osmotic pressure gradient (e.g. by polyethylene glycol, PEG 6000; reflection coefficient $\sigma = 1$; [31]) is generated across the alginate membrane separating the two compartments, the osmotic permeability, P_f, of the matrix can be calculated from the water flow J_v according to $P_f = J_v RT/(\pi V_w)$, with R = gas constant, T = absolute temperature in Kelvin, π = osmotic pressure of the osmolyte solution, V_w = molar volume of water [32]. Prerequisite is that the water efflux from the water-filled compartment, b, is equal to the water influx into the osmolyte-containing compartment, a (see data in Fig. 7). At present data are only available for alginate membranes cross-linked by external Ba^{2+}. For these membranes P_f values of about 2×10^{-2} cm/s were calculated from transmembrane water flow data. In contrast, the diffusive permeability of water, P_D, of the 1-mm thick alginate matrix ($P_D = D_w/d \approx 2.4 \times 10^{-4}$ cm/s) is about 100 times smaller (the diffusion coefficient of water, D_w, in cross-linked alginate can easily be determined by ^{1}H-PGSE-NMR measurements; [33]). This finding provides clear-cut evidence [34] that water moves by viscous flow, i.e. through pores, rather than by diffusion. Assuming that the flow is laminar, the "equivalent pore radius", r, [35] can be estimated from the P_f/P_D ratio using the equation $P_f/P_D = r^2 RT/(8\eta D_w V_w)$, with η = viscosity of water [36]. Calculations yield an equivalent pore radius of about 4 nm (at room temperature). This is consistent with the finding that immunologically relevant proteins, which have an effective molecular radius of about 7.5 nm [37], are excluded from the passage through the alginate pores whereas smaller molecules like insulin (1.5–4 nm; [37]) can freely pass the alginate barrier.

Measurements with alginate membranes cross-linked by the "crystal gun" method are planned. Independent of the outcome of these experiments it is clear from the above considerations that measurement of water (and also of solute) permeability through 2-D-alginate matrices yields valuable information for the assessment of microcapsule permeability while keeping the mechanical stability at an optimum value. This is because the data obtained on the 2-D matrices can easily be extrapolated to the small-sized microcapsules.

6. Animal trials

The improvements in purification of alginates and in encapsulation as well as the development of various validation protocols paves the way for long term

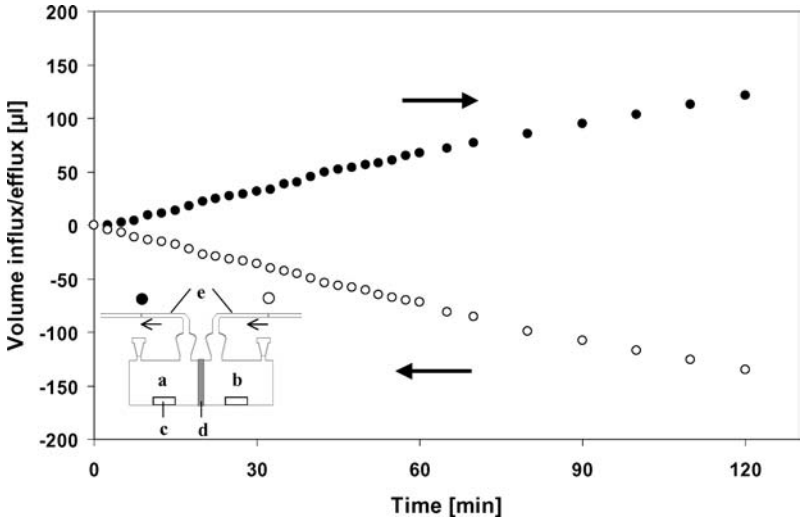

Figure 7 Osmotically-induced water flow across a 1-mm thick, planar alginate membrane of circular size (diameter 20 mm, 0.7% w/v *L. nigrescens* alginate, cross-linked with external Ba^{2+}) at room temperature. The experimental setup (see inset) consisted of two glass chambers "a" (containing 290 mM PEG 6000) and "b" (containing distilled water), each having a circular face with a 13-mm-diameter hole in it in which the alginate membrane ("d" in inset; integrated in a teflon support and stabilized by nylon nets) was clamped to form a fluid tight seal. Osmotically induced water flow occurred through the alginate membrane. Vigorous stirring in the bulk phases by small magnetic stirrers (c) minimized unstirred layer effects. Transmembrane water flow was determined by monitoring the movement of the menisci in the rectangular bent capillaries attached to the glass chambers ("e" in inset; → water influx into compartment "a", ← water efflux from compartment "b"). Note that the numerical slope of water influx and efflux are almost identical, as expected when there is no water loss. Note further that diffusive water flow around the alginate membrane can be excluded because no PEG 6000 could be detected in the water-filled compartment "b" after the end of the experiment.

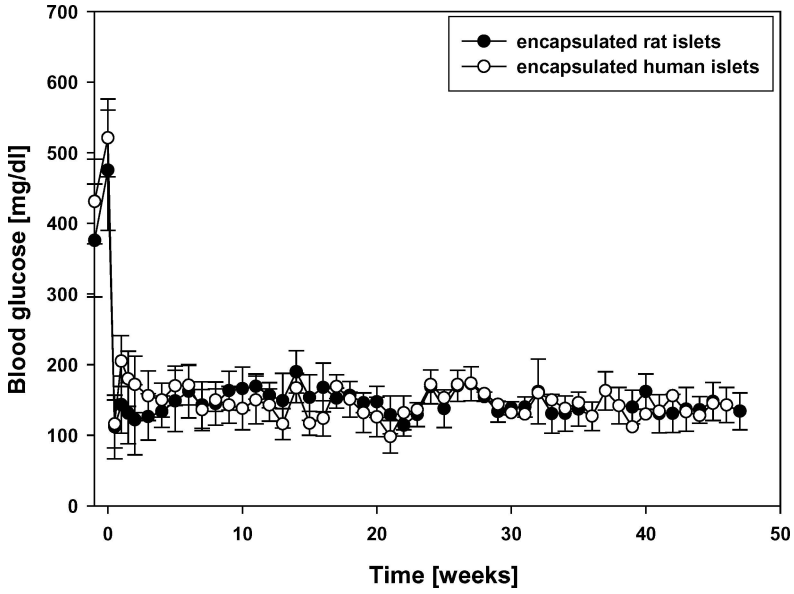

Figure 8 Long-term graft function of alginate-encapsulated rat ($n = 5$) as well as human ($n = 2$) islets transplanted into diabetic Balb/c mice (mean ± SE); transplantation at $t = 0$.

transplantation studies. As shown in Fig. 8 encapsulated rat as well as human islets reversed chemically-induced diabetes in mice over extremely long times (experiments still continue) without the need for administration of immunosuppressives. These findings are confirmed by intraperitoneal glucose tolerance tests (IPGTTs) and *in vitro* testing of explanted microcapsules. The microcapsules showed normal regulation of insulin secretion upon glucose challenge. Furthermore, no significant fibrosis was observed on the surface of explanted, islet-containing microcapsules 10 or 36 weeks after transplantation [38].

The peritoneum was selected as the site of xenograft transplantation. However, the preferred sites, at least for the first clinical applications, are muscle pockets, e.g. in the non-dominant forearms and in the back because oxygen concentration is high and in the case of graft failure, microcapsules can be retrieved easily. A further advantage is that location of the microcapsules and their internal oxygen concentration can be monitored non-invasively by ^{19}F-NMR-imaging [3, 4]. However, the mechanical forces here are significant resulting ultimately in fibrotic overgrowth and/or microcapsule breakage as demonstrated by failure of parathyroid transplants in the pilot clinical trial [5]. It is expected that encapsulated islets will have as long a lifetime in muscle pockets as in the peritoneum provided that the microcapsule design technology developed in recent

years is fully implemented. Especially useful may be the "crystal gun" method and the very recent finding that microcapsules made up of a 1:1 mixture of *L. nigrescens* and *L. trabeculata* alginate are extremely stable under *in vitro* conditions (see above) and do not provoke any inflammatory or fibrotic response.

7. Cryopreservation technology and validation

Considering the successful animal transplantation studies and the large body of recent microcapsule design technology, cryopreservation of encapsulated islets (or other cells) is becoming a focus of research because just-in-time manufacturing of alginate-immunoprotected islets (or other cells and tissues) is difficult to implement. Quality control, and the creation of archives for validation of the manufacturing process of the alginates and the microcapsules also require the long-term storage of the final transplants. Although progress in developing cryopreservation procedures for cells is encouraging [39, 40], many challenges remain because of the scale and complexity of tissues resulting in spatial, thermal, chemical, and osmotic (mechanical) gradients throughout the system during the freezing or subsequent thawing processes. Membrane permeating (e.g. glycerol and dimethyl sulfoxide, DMSO) and nonpermeating (e.g. hydroxyethyl starch, trehalose, inositol) cryoprotectants are usually added before freezing in order to increase the number of viable cells recovered after thawing. DMSO is the most commonly used cryoprotectant. However, DMSO may be cytotoxic, particularly if the time of exposure before freezing and after thawing is long, or if it is used in high concentrations (usually up to 20%), precluding medical approval. Reduction of the DMSO concentration or complete replacement of DMSO by equally powerful, but medically approved substances as well as technical improvements to the freezing and thawing process are the current strategies for overcoming the problems of cryopreservation of tissue.

The most promising technical improvements of the freezing process are the significant reduction of total sample volume, i.e. miniaturization of the cryosubstrates from typical 1 millilitre down to microlitres or below. The main advantages for the storage of encapsulated and non-encapsulated tissue are the avoidance of large temperature gradients and inhomogeneities [41]. The reduced temperature gradients in the smaller cryosubstrates arise from the thermal conductivity of

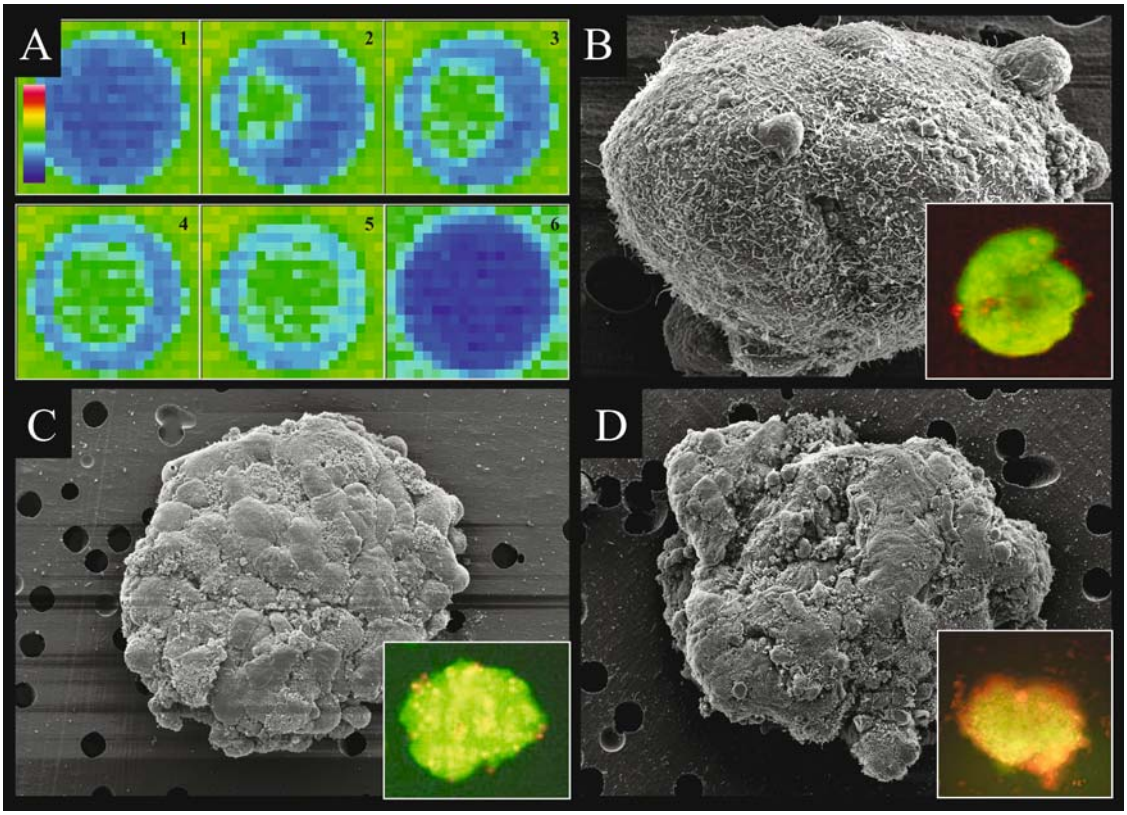

Figure 9 Freezing of Langerhans islets in micro-well-plates made from high-density polyethylene (HDPE). (A) Successive frames of a single well at the time of ice growth made with infrared thermography. The temperature rise associated with transition from supercooled liquid (frames 2 to 4) to a 2-phase system (with release of latent heat) can be seen in the 5th frame and is complete in the 6th frame. Note that the temperature scale given in (A) reached from $+30\,^{\circ}$C (red) to $-30\,^{\circ}$C (blue). Note that the time delay between the frames is different (1→2 640 ms, 2→3 160 ms, 3→4 160 ms, 4→5 640 ms, 5→6 132 s). (B) Langerhans islet. Scanning electron microscopy (SEM) of a control preparation. The islets were placed on Millipore^{TM} filter inserts. Note the surface texture. Horizontal field width (HFW) = 92 μm. Bottom right: Cell viability assessed by double staining with fluorescein diacetate (green fluorescence for intact cells) and ethidium bromide (red fluorescence for nuclei of damaged cells). The cell viability test (bottom right) showed about 87% viability. (C) SEM of Langerhans islet immediately after cryopreservation in HDPE–micro-well-plate with 7% DMSO. Note the smooth, undamaged surface. HFW = 184 μm. A cell viability test (bottom right) showed about 64% viability. (D) SEM of Langerhans islet immediately after cryopreservation in HDPE–micro-well-plate with 14% DMSO. Note the smooth surface with areas of damage. HFW = 184 μm. A cell viability test (bottom right) showed about 43% viability.

water, that becomes, though small, increasingly important in determining heat flows with decreasing sample size. Thus, either higher freezing rates or more homogeneous freezing of the sample are possible. A further advantage of small-sized cryosubstrates is the possibility of fast and exact addition of cryoprotectant additives by pipette robots. Fast addition results in an immediate and homogeneous distribution of the cryoprotectants. Non-encapsulated islets cryopreserved in this way were highly functional after thawing even though significantly lower final concentrations of DMSO than usual were applied before freezing. For quality control of transplants it is an extremely important advantage that the surface temperature of the sample volume during the freezing and thawing process can directly be observed by dynamic high-resolution thermo imaging (Fig. 9).

Parallel to these promising advances in technology, novel media for the cryopreservation of islets (and other mammalian cells) have been developed [42]. The DMSO-free media are hypotonic (150 mOsm) and contain appropriate amounts of trehalose and/or inositol as major osmolytes. Mammalian cells (including islets) respond to hypotonic challenge by swelling until a maximum volume is reached after 3–5 min (Fig. 10). In the presence of trehalose, but not of inositol a regulatory volume decrease (RVD) is observed. According to the literature [43] swelling activates Cl^- channels. Efflux of Cl^- leads to a depolarization of the membrane. This evokes activation of K^+ channels. Thus, restoration of the original volume after about 15 min is accomplished by release of intracellular KCl and water. While the K^+ channels are selective, the Cl^- channels allow the passage of other anions as well as of inositol (and other cryoprotectant monomeric sugar alcohols). In the presence of inositol the volume of the swollen cells remains constant or even increases slightly (Fig. 10) indicating that KCl efflux is compensated by inositol uptake. Cryopreservation of islets pre-loaded hypotonically with inositol and incubated in isotonic trehalose have yielded high survival rates after thawing. A few dead cells (detected by propidium iodide staining under the cryomicroscope) were seen occasionally in the periphery of the islets. Adoption of the technology described above to these media should lead to further improvements in cryopreservation.

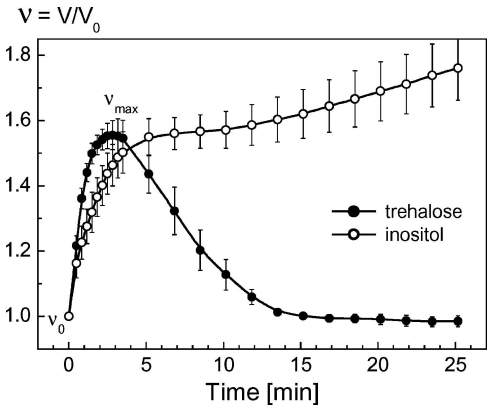

Figure 10 Temporal changes in the relative volume, ν, of rat islets of Langerhans in hypotonic 150 mOsm media containing inositol (open circles) or trehalose (filled circles) as the major osmolyte. The islets were originally ($t < 0$) exposed to an isotonic saline solution (300 mOsm). At zero time the islets were rapidly transferred into a hypotonic sugar solution. After fast initial swelling (3–5 min), the islets either exhibited regulatory volume decrease (RVD, trehalose) or underwent slow secondary swelling (inositol). The lack of RVD in the inositol medium indicates that cell swelling rendered the membrane of islet cells highly permeable to inositol (unlike the case for trehalose). Islet volumes, V, were calculated from their microscopic cross-sectional areas by assuming spherical geometry. The relative islet volume is defined as $\nu = V/V_0$, where V and V_0 are the cell volume and the initial (isotonic) volume, respectively. Each data point represents the mean ± SE of three independent measurements.

8. Conclusions

Even though significant advances have obviously been made in immunoisolated transplantation, many challenges remain. Amongst these is, most importantly, the development of closed microfluidics platforms allowing automation of the microencapsulation process. Incorporating the entire process steps, from alginate/cell droplet formation, cross-linking by injection of Ba^{2+} nanoparticles to microcapsule validation, in a chip-based platform (microlab) should meet the GMP standards and demands for routine clinical applications of encapsulated cells and tissues as well as for controlled drug release. Together with this, the advanced cryotechnology described here must be extended to alginate-encapsulated tissues (islets) in order to meet the demands of the granting agencies for long-term storage of transplants. The extremely high water content of alginate gels and the large component of bound water [44] pose enormous problems, but advances in micro- and nanotechnology offer a broad spectrum of solutions. Potential solutions can additionally be found among drought- and freezing-resistant and -tolerant plants as shown recently [45–47].

The remaining challenges are tremendous, but the significant advances described here were made by interdisciplinary research activities. Therefore, we are confident that close interdisciplinary collaboration will find solutions to the outstanding problems.

Acknowledgments

These studies were supported by grants from Deutsche Forschungsgemeinschaft (Zi 99/15-1 to U.Z.), BMBF (16 SV 1329 and 0311 588 to U.Z.; 16 SV 1366/0 and O3N8707 to H.Z.), Forum (AZ 437-2004 to S. S.), and research grants of Novo Nordisk Pharma GmbH, Germany, and the Stiftung Rheinland-Pfalz für Innovation (386261/525 to M.M.W. and S.S.) as well as by FONDECYT (1000044 to J.A.V.).

References

1. W. M. KÜHTREIBER, R. P. LANZA and W. L. CHICK, in "Cell Encapsulation Technology and Therapeutics" (Birkhäuser, Boston, 1999).
2. R. P. LANZA, R. LANGER and J. VACANTI, in "Principles of Tissue Engineering" (Academic Press, San Diego, 2000).
3. U. ZIMMERMANN, S. MIMIETZ, H. ZIMMERMANN, M. HILLGÄRTNER, H. SCHNEIDER, J. LUDWIG, C. HASSE, A. HAASE, M. ROTHMUND and G. R. FUHR, *BioTechniques* **29**(3) (2000) 564.

4. U. ZIMMERMANN, F. THÜRMER, A. JORK, M. WEBER, S. MIMIETZ, M. HILLGÄRTNER, F. BRUNNENMEIER, H. ZIMMERMANN, I. WESTPHAL, G. R. FUHR, U. NÖTH, A. HAASE, A. STEINERT and C. HENDRICH, *Ann. N.Y. Acad. Sci.* **944**(1) (2001) 199.
5. C. HASSE, G. KLÖCK, A. SCHLOSSER, U. ZIMMERMANN and M. ROTHMUND, *Lancet* **350**(9087) (1997) 1296.
6. T. G. WANG, in "Cell Encapsulation Technology and Therapeutics," edited by W. M. Kühtreiber, R. P. Lanza and W. L. Chick (Birkhäuser, Boston, 1999) p. 29.
7. H. ZIMMERMANN, M. HILLGÄRTNER, B. MANZ, P. J. FEILEN, F. BRUNNENMEIER, U. LEINFELDER, M. WEBER, H. CRAMER, S. SCHNEIDER, C. HENDRICH, F. VOLKE and U. ZIMMERMANN, *Biomaterials* **24**(12) (2003) 2083.
8. B. H. A. REHM, in "Biopolymers: Polysaccharides I: Polysaccharides from Prokaryotes," edited by E. J. Vandamme, S. De Baets and A. Steinbüchel (Wiley-VCH, Weinheim, 2002) Vol. 5, p. 179.
9. K. I. DRAGET, O. SMIDSRØD and G. SKJÅK-BRÆK, in "Biopolymers: Polysaccharides II: Polysaccharides from Eukaryotes," edited by S. De Baets, E. J. Vandamme and A. Steinbüchel (Wiley-VCH, Weinheim, 2002) Vol. 6, p. 215.
10. J. A. VÁSQUEZ, in "Coastal Plant Communities of Latin America," edited by U. Seeliger (Academic Press, San Diego, 1992) p. 77.
11. M. VENEGAS, B. MATSUHIRO and M. E. EDDING, *Botanica Marina* **36** (1993) 47.
12. U. LEINFELDER, F. BRUNNENMEIER, H. CRAMER, J. SCHILLER, K. ARNOLD, J. A. VÁSQUEZ and U. ZIMMERMANN, *Biomaterials* **24**(23) (2003) 4161.
13. B. MATTIASSON, in "Immobilized Cells and Organelles," edited by B. Mattiasson (CRC Press, Boca Raton, 1983) Vol. I, p. 3.
14. M. DORNISH, D. KAPLAN and Ø. SKAUGRUD, *Ann. N.Y. Acad. Sci.* **944**(1) (2001) 388.
15. M. A. ATKINSON and E. H. LEITER, *Nat. Med.* **5**(6) (1999) 601.
16. J. WIJSMAN, P. ATKISON, R. MAZAHERI, B. GARCIA, T. PAUL, J. VOSE, G. O'SHEA and C. STILLER, *Transplantation* **54**(4) (1992) 588.
17. U. ZIMMERMANN, C. HASSE, M. ROTHMUND and W. KÜHTREIBER, in "Cell Encapsulation Technology and Therapeutics," edited by W. M. Kühtreiber, R. P. Lanza and W. L. Chick (Birkhäuser, Boston, 1999) p. 40.
18. C. RYSER, J. WANG, S. MIMIETZ and U. ZIMMERMANN, *J. Membr. Biol.* **168**(2) (1999) 183.
19. M. HEIDECKER, S. MIMIETZ, L. H. WEGNER and U. ZIMMERMANN, *J. Membr. Biol.* **192**(2) (2003) 123.
20. M. HILLGÄRTNER, H. ZIMMERMANN, S. MIMIETZ, A. JORK, F. THÜRMER, H. SCHNEIDER, U. NÖTH, C. HASSE, A. HAASE, G. R. FUHR, M. ROTHMUND and U. ZIMMERMANN, *Math.-Wiss. u. Werkstofftech.* **30** (1999) 783.
21. S. SCHNEIDER, P. J. FEILEN, H. CRAMER, M. HILLGÄRTNER, F. BRUNNENMEIER, H. ZIMMERMANN, M. M. WEBER and U. ZIMMERMANN, *J. Microencapsul.* **20**(5) (2003) 627.
22. U. ZIMMERMANN, H. CRAMER, A. JORK, F. THÜRMER, H. ZIMMERMANN, G. R. FUHR, C. HASSE and M. ROTHMUND, in "Biotechnology," edited by H. J. Rehm and G. Reed (Wiley-VCH, Weinheim, 2001) Vol. 10, p. 547.
23. B. THU, O. GASEROD, D. PAUL, A. MIKKELSEN, G. SKJÅK-BRÆK, R. TOFFANIN, F. VITTUR and R. RIZZO, *Biopolymers* **53**(1) (2000) 60.
24. B. MANZ, M. HILLGÄRTNER, H. ZIMMERMANN, D. ZIMMERMANN, F. VOLKE and U. ZIMMERMANN, *Eur. Biophys. J.* **33**(1) (2004) 50.
25. R. WOLF, *J. Microsc.* (*London*) **153** (1989) 181.
26. R. WOLF, in "Science, Technology and Education of Microscopy: an Overview," edited by A. Mendez-Vilas (Formatex, Madrid, 2003) p. 720.
27. O. SMIDSRØD and G. SKJÅK-BRÆK, *Trends Biotechnol.* **8**(3) (1990) 71.
28. C. DULIEU, D. PONCELET and R. J. NEUFELD, in "Cell Encapsulation Technology and Therapeutics," edited by W. M. Kühtreiber, R. P. Lanza and W. L. Chick (Birkhäuser, Boston, 1999) p. 3.
29. P. B. MESSERSMITH and S. STARKE, *Chem. Mater.* **10**(1) (1998) 117.
30. M. E. WESTWOOD and P. J. THORNALLEY, in "The Glycation Hypothesis of Atherosclerosis," edited by C. Colaco (Landes Bioscience, Georgetown, 1997) p. 57.
31. U. ZIMMERMANN and E. STEUDLE, *Adv. Bot. Res.* **6** (1978) 45.
32. J. DAINTY, *Adv. Bot. Res.* **1** (1963) 279.
33. E. O. STEJKAL and J. E. TANNER, *J. Chem. Phys.* **42** (1965) 288.
34. M. MAURO, *Science* **126** (1957) 252.
35. A. K. SOLOMON, *J. Gen. Physiol.* **51**(5) (1968) 335.
36. E. ROBBINS and A. MAURO, *ibid.* **43**(3) (1960) 523.
37. F. J. MARTIN and C. GROVE, *Biomed. Microdiv.* **3**(2) (2001) 97.
38. S. SCHNEIDER, P. J. FEILEN, F. BRUNNENMEIER, U. ZIMMERMANN and M. M. WEBER, *Diabetes* **53**(2) (2004) A 615.
39. J. H. CROWE and L. M. CROWE, *Nat. Biotechnol.* **18**(2) (2000) 145.
40. A. EROGLU, M. J. RUSSO, R. BIEGANSKI, A. FOWLER, S. CHELEY, H. BAYLEY and M. TONER, *Nat. Biotechnol.* **18**(2) (2000) 163.
41. H. ZIMMERMANN, A. D. KATSEN, F. R. IHMIG, CH. H. P. DURST, ST. G. SHIRLEY and G. R. FUHR, *IEE Proc. Nanobiotechnol.* **151**(4) (2004) 134.
42. R. REUSS, J. LUDWIG, R. SHIRAKASHI, F. EHRHART, H. ZIMMERMANN, S. SCHNEIDER, M. M. WEBER, U. ZIMMERMANN, H. SCHNEIDER and V. L. SUKHORUKOV, *J. Membr. Biol.* **200**(2) (2004) 67.
43. F. LANG, G. L. BUSCH and H. VÖLKL, *Cell. Physiol. Biochem.* **8**(1/2) (1998) 1.
44. M. ESCH, V. L. SUKHORUKOV, M. KÜRSCHNER and U. ZIMMERMANN, *Biopolymers* **50**(3) (1999) 227.
45. H. SCHNEIDER, N. WISTUBA, H. J. WAGNER, F. THÜRMER and U. ZIMMERMANN, *New Phytol.* **148**(2) (2000) 221.
46. H. SCHNEIDER, B. MANZ, M. WESTHOFF, S. MIMIETZ, M. SZIMTENINGS, T. NEUBERGER, C. FABER, G. KROHNE, A. HAASE, F. VOLKE and U. ZIMMERMANN, *New Phytol.* **159**(2) (2003) 487.
47. H. J. WAGNER, H. SCHNEIDER, S. MIMIETZ, N. WISTUBA, M. ROKITTA, G. KROHNE, A. HAASE and U. ZIMMERMANN, *New Phytol.* **148**(2) (2000) 239.

Received 15 August
and accepted 15 October 2004